JACS
JOURNAL OF THE AMERICAN CHEMICAL SOCIETY

ARTICLE

pubs.acs.org/JACS

Molecular Trapping on Two-Dimensional Binary Supramolecular Networks

Yu Li Huang,[†] Wei Chen,[*,†,‡] and Andrew Thye Shen Wee[*,†]

[†]Department of Physics, National University of Singapore, 2 Science Drive 3, 117542, Singapore

[‡]Department of Chemistry, National University of Singapore, 3 Science Drive 3, 117543, Singapore

Supporting Information

ABSTRACT: Molecular preferential adsorption on molecular patterned surfaces via specific intermolecular interactions provides an efficient route to construct ordered organic nanostructures for future nanodevices. Here, we demonstrate the preferential trapping of second-layer molecules atop two-dimensional binary supramolecular networks, F_{16}CuPc on DIP: F_{16}CuPc and 6P:F_{16}CuPc systems, respectively, through intermolecular $\pi-\pi$ interactions. The formation of the second-layer supramolecular nanostructures, individual molecular dots or linear molecular chains, can be controlled by the underlying molecular networks.

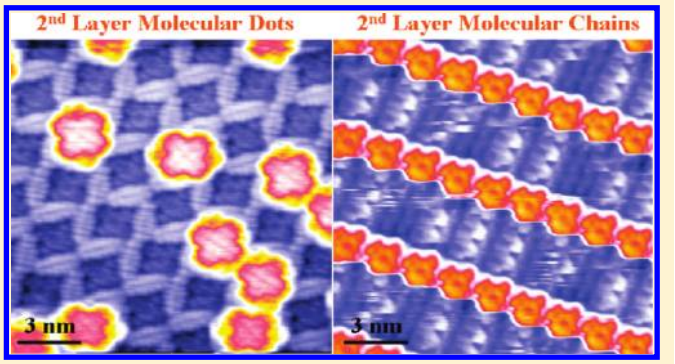

INTRODUCTION

Selective coupling of functional molecules at special adsorption sites on surface nanotemplates represents a promising route to fabricate ordered organic nanostructure arrays with desired functionality over macroscopic areas for molecular nanodevice applications.[1−6] Several groups have reported the development of two-dimensional (2D) nanoporous surface nanotemplates, which can provide geometrical voids to trap molecules.[1−15] Examples include the boron nitride (BN) nanomesh,[7,8] carbon nanomesh on silicon carbide (SiC),[9] and supramolecular nanoporous surface templates constructed via metal−ligand bonding,[10] multiple intermolecular hydrogen-bonding,[11−14] or other noncovalent intermolecular interactions.[15−17] Such selective trapping of molecules can also be realized through molecular recognition on preferential binding sites on molecular surface nanotemplates via specific noncovalent intermolecular interactions.[18−23] The trapping of second-layer molecules (or atoms) on specific adsorption sites of a nonporous planar molecular surface nanotemplate, instead of using a porous nanotemplate, has been rarely reported.[23,24] As 2D supramolecular networks with two or more components can offer different molecular adsorption positions, they have great potential to be used as nanotemplates to facilitate the growth of molecular nanostructures with designed 2D arrangements. In order to preserve the patterns of the underlying molecular networks as well as the pristine unique properties of the trapped functioning molecules during the assembling processes, stabilizing the trapped molecules using selective and nonchemical intermolecular interactions (such as intermolecular $\pi-\pi$ interaction) is highly desired.

The formations of well-defined planar molecular networks constructed from multiple components over macroscopic areas have been widely reported in recent years.[19,23,25−27] By rational design and selection of molecular building blocks, it is possible to fabricate various molecular arrays with desired functionality, as well as supramolecular packing structure, such as 1D molecular chain arrays,[28−30] 2D chessboard-like structures,[31,32] hexagonal networks,[19,23] and so on, and hence to control the formation of the top-layer nanostructures. In this report, molecular trapping via intermolecular $\pi-\pi$ interactions on binary molecular networks is demonstrated by the assembly of copper hexadecafluorophthalocyanine (F_{16}CuPc) molecules on hydrogen-bonded binary molecular networks of F_{16}CuPc with di-indenoperylene (DIP) and F_{16}CuPc with *p*-sexiphenyl (6P) on graphite.[26] These π-conjugated planar organic molecules, F_{16}CuPc, DIP, and 6P, are potential candidates in bulk heterojunction photovoltaic cells or as controlled injection barriers in organic thin-film devices.[33,34] The second-layer F_{16}CuPc molecules exclusively adsorb atop the same type of molecules in the underlying binary molecular network mainly via intermolecular $\pi-\pi$ interactions, resulting in the formation of F_{16}CuPc molecular dots or chain arrays.

EXPERIMENTAL SECTION

The experiment was carried out in a multichamber ultra-high-vacuum (UHV) system housing an Omicron low-temperature scanning tunneling microscopy (LT-STM) interfaced to a Nanonis controller.[22,23,33] Our STM experiments were performed in constant-current mode, and the tunneling current applied for *in situ* imaging is usually in the range of 60−100 pA. All the STM images were captured at 77 K. Freshly cleaved highly oriented

Received: July 17, 2010
Published: December 27, 2010

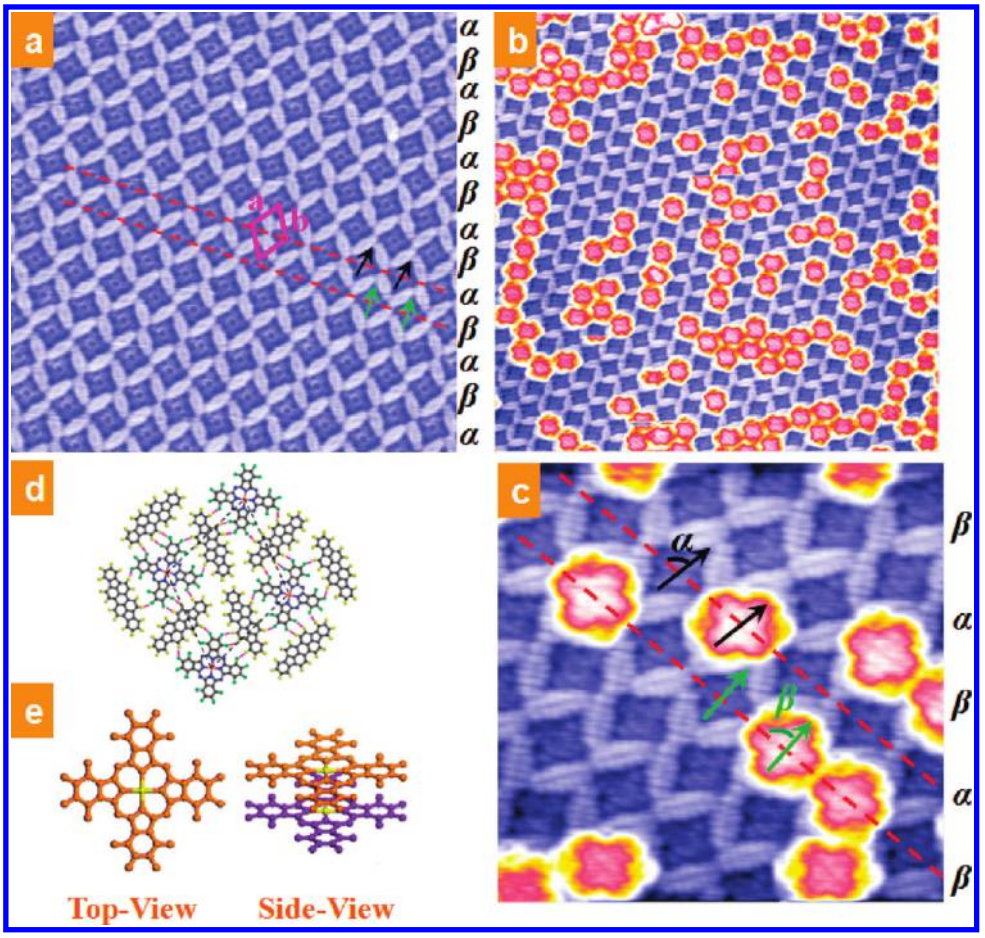

Figure 1. (a) 30 × 30 nm^2 STM image (V_{tip} = 2.2 V) showing the DIP:F_{16}CuPc network at the ratio of 2:1, where each F_{16}CuPc molecule is surrounded by four DIP molecules, and (d) its corresponding simulated supramolecular structure. (b) Deposition of 0.16 ML F_{16}CuPc onto the network results in the random decoration of isolated F_{16}CuPc molecules on this network (50 × 50 nm^2, V_{tip} = 1.9 V). (c) A zoom-in 15 × 15 nm^2 image of panel b reveals that the top F_{16}CuPc exclusively perches on top of the underlying F_{16}CuPc molecular site in the binary molecular network (V_{tip} = 2.0 V). (e) Top- and side-view schematic drawings of the packing structure.

pyrolytic graphite (HOPG) substrate was thoroughly degassed in UHV at around 800 K overnight before deposition. 6P, DIP, and F_{16}CuPc were sequentially deposited from Knudsen cells onto HOPG at room temperature in a separate growth chamber. Prior to the deposition, all molecular sources were purified twice by gradient vacuum sublimation. The deposition rates of 6P (0.01 ML min^{-1}), DIP (0.01 ML min^{-1}), and F_{16}CuPc (0.03 ML min^{-1}) were monitored by a quartz crystal microbalance during evaporation and were further calibrated by counting the adsorbed molecule coverage in large-scale LT-STM images at coverages below 1 monolayer (1 ML = one full monolayer of closely packed 6P, DIP, or F_{16}CuPc with their conjugated π-plane oriented parallel to HOPG surface).

■ RESULTS AND DISCUSSION

1. Second-Layer Molecular Dots atop DIP:F_{16}CuPc Binary Network. Figure 1a shows the molecularly resolved 30 × 30 nm^2 STM image of the DIP:F_{16}CuPc network, where the four-leaved pattern represents a F_{16}CuPc molecule and the bright leaf-like feature represents a single DIP molecule. The DIP:F_{16}CuPc molecular ratio is 2:1 for this network.[26] Each F_{16}CuPc molecule is surrounded by four DIP molecules to maximize the intermolecular interactions (i.e., the C−F···H−C hydrogen-bonding between the periphery F atoms on F_{16}CuPc and H atoms on neighboring DIP molecules), thereby ensuring good structural stability of this binary molecular network.[26,35] The primitive cell of the template is indicated by a rhombus in Figure 1a, with dimensions of a = 2.66 ± 0.02 nm, b = 2.70 ± 0.02 nm, and θ = 66° ± 2°. Thus, this molecular template can be considered as a network with a quasi-three-fold symmetry, with $a \approx b \approx 2.68$ nm and $\theta \approx 60°$ (see details in Supporting Information). Along the short diagonal direction of the primitive cell (dashed lines), the F_{16}CuPc molecules possess the same in-plane orientation in each molecular row, with a periodicity of 2.88 ± 0.02 nm, while in the direction perpendicular to the dashed line, the molecular in-plane orientations alternate between α = 95° ± 2° and β = 85° ± 2°, as denoted by the arrows in Figure 1a. The supramolecular model based on molecular dynamic simulation is shown in Figure 1d.[26] The possible hydrogen bonds with F···H distances shorter than 2.6 Å are highlighted by pink lines in the simulated model.[26]

Further deposition of F_{16}CuPc results in a disordered decoration of individual molecules on this molecular template. As shown in Figure 1b, at coverage of 0.16 ML, the second-layer F_{16}CuPc molecules adsorbing atop the DIP:F_{16}CuPc template appear as four-lobe-like protrusions (in orange), and no long-range ordering is observed. The zoom-in 15 × 15 nm^2 image in Figure 1c clear demonstrates that each F_{16}CuPc molecule in the second layer precisely adsorbs on top of the underlying F_{16}CuPc molecule. The second-layer molecule possesses α or β in-plane orientation the same as its underlying one, as denoted by the

dx.doi.org/10.1021/ja106350d |J. Am. Chem. Soc. 2011, 133, 820–825

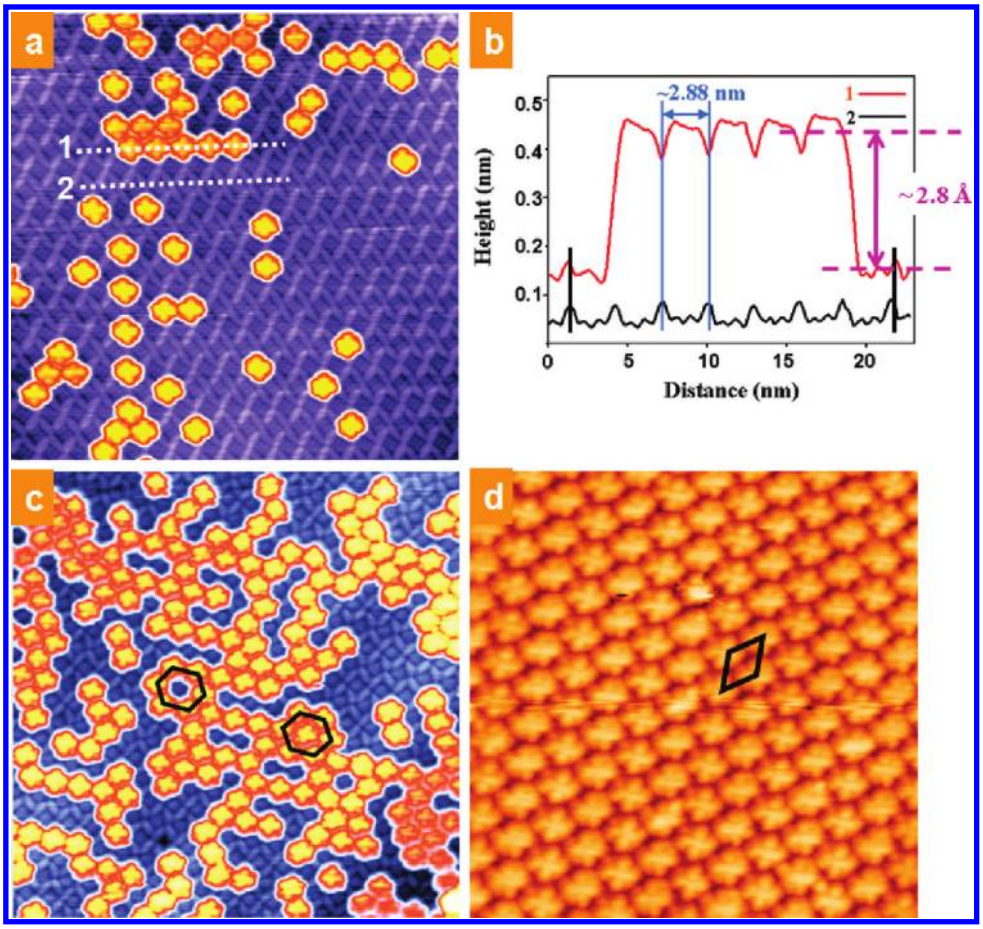

Figure 2. The DIP:F_{16}CuPc networks are decorated by different amounts of F_{16}CuPc: (a) ~0.06 ML (50 × 50 nm^2, V_{tip} = 2.0 V), (c) ~0.2 ML (50 × 50 nm^2, V_{tip} = 2.7 V), and (d) ~0.4 ML (30 × 30 nm^2, V_{tip} = 2.5 V). (b) The line profiles corresponding to the dashed lines 1 and 2 in panel (a) reveal the same 2.88 nm periodicity of the second-layer molecular arrays and the underlying network. The short black lines show that these two lines have the same starting and ending points, while the blue lines indicate that the first- and second-layer F_{16}CuPc are coaxially aligned.

arrows in Figure 1c. There is no visible lateral displacement between the first- and second-layer molecules (see details in Supporting Information). The proposed stacking structure is demonstrated in the schematic drawing in Figure 1e, where the purple molecules represent the first-layer F_{16}CuPc (underlying) and the orange ones represent the second-layer molecules. The populations of the second-layer molecules adopting α or β orientation are nearly equivalent (analyzed over 1000 molecules), suggesting that the underlying α and β adsorption sites have the same surface energy potential.

To confirm the observed packing geometry, we further analyze the formation of the second-layer F_{16}CuPc molecular arrays at various coverages, 0.06, 0.2, and 0.4 ML, in Figure 2a, c, and d, respectively. In Figure 2a, the molecularly resolved STM image shows the DIP:F_{16}CuPc network decorated with ~0.06 ML F_{16}CuPc, where the dashed line 1 is taken along the second-layer molecular arrays and line 2 along the template. As revealed in the line profiles of Figure 2b, the height difference between the four-lobe-like protrusions and the underlying template is about 2.8 Å (line 1), confirming that these protrusions are attributed to second-layer F_{16}CuPc molecules. It also reveals that the lines 1 and 2 have the same 2.88 ± 0.02 nm periodicity along the short diagonal direction of the primitive cell of the underlying template, and the protrusions of line 1 (corresponding to the second-layer F_{16}CuPc) are coaxially aligned with the pits of line 2 (the first-layer F_{16}CuPc), as indicated by the blue lines in Figure 2b. That is, the second-layer F_{16}CuPc molecules precisely sit atop the underlying ones, with their central copper atoms coaxially aligned (see details in Supporting Information). From large-scale STM images, no long-range ordered, closely packed aggregation of the second-layer F_{16}CuPc molecules is observed when the coverage is not higher than ~0.2 ML (Figure 2c). Correspondingly, as indicated by the quasi-hexagons in Figure 2c, the intermolecular distance between the nearest-neighboring second-layer molecules is around 2.68 nm, reminiscent of the underlying network ($a \approx b \approx 2.68$ nm). When the amount of the second-layer F_{16}CuPc increases to ~0.4 ML, a loosely packed F_{16}CuPc molecular array is formed on the template, as all the first-layer adsorption sites have been occupied. As denoted by the rhombus in Figure 2d, the primitive cell of the second-layer F_{16}CuPc array has the same dimensions as the underlying template.

The stacking geometry in which the second-layer F_{16}CuPc is precisely perched atop the underlying layer is in contradiction with previously reported multilayer metal phthalocyanine thin films (such as F_{16}CuPc and FePc), which usually adopt slipped or rotated stacking geometries to maximize interlayer $\pi-\pi$ interactions.[36−39] An unusual coaxial stacking structure of a CoPc bilayer on a Cu(111) surface has been reported by Berndt et al., which is attributed to the additional Co−Co binding between the first- and second-layer CoPc molecules.[40] We suggest that the formation of the unique stacking geometry of the second-layer F_{16}CuPc here is due to the

dx.doi.org/10.1021/ja106350d |J. Am. Chem. Soc. 2011, 133, 820–825

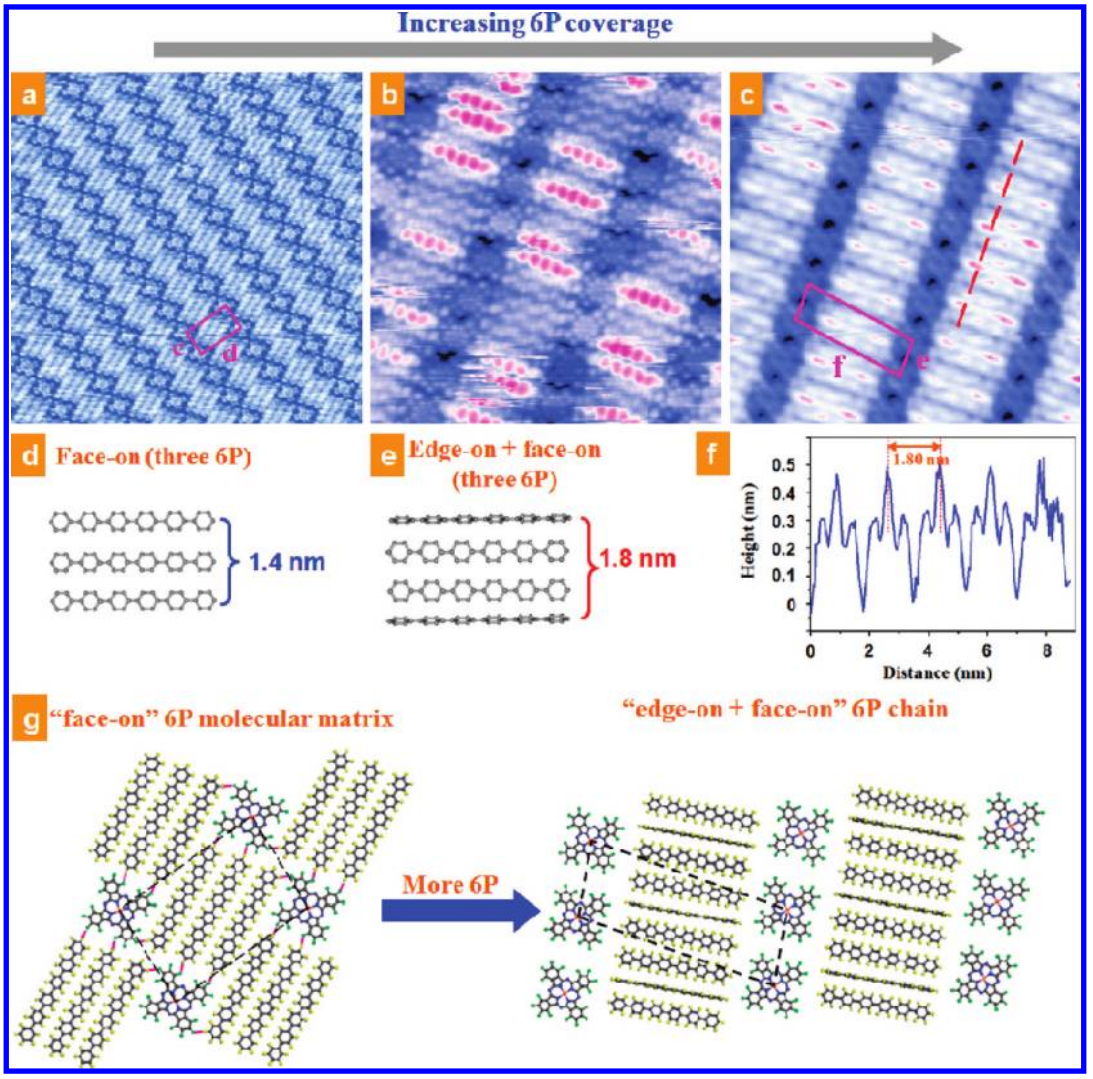

Figure 3. (a) 30 × 30 nm^2 STM image showing the perfectly ordered oblique F_{16}CuPc molecular dot array comprising two F_{16}CuPc doublets interlinked by a 6P triplet with 6P:F_{16}CuPc = 3:1 (V_{tip} = 2.7 V). (b) Insertion (randomly) of the edge-on 6P molecules into face-on 6P molecules results in the transition to a F_{16}CuPc linear chain array (15 × 15 nm^2, V_{tip} = 2.5 V). (c) F_{16}CuPc linear chain array interconnected by an ordered "edge-on + face-on" 6P molecular wire (15 × 15 nm^2, V_{tip} = 2.6 V). (d,e) Schematic drawings of the molecular packing structures of the face-on 6P triplet and the "edge-on + face-on" 6P chain, respectively. (f) The line profile taken along the "edge-on + face-on" 6P chain as marked by the dashed line in panel c, revealing a 1.8 nm periodicity. (g) Proposed corresponding supramolecular packing structure transition from panel (a) to panel (c).

geometrical confinement of the underlying DIP:F_{16}CuPc network, as no similar phenomenon was found either on the bilayer F_{16}CuPc film on HOPG[36] or on the second-layer F_{16}CuPc stripes on the 6P:F_{16}CuPc network discussed in the following. Furthermore, the overall arrangement of the second-layer molecular arrays was investigated (detailed statistical results are shown in the Supporting Information), and we did not observe any long-range ordering of the molecular distribution before the underlying template was fully covered. Such formation of second-layer molecular arrays without long-range ordering at coverage not higher than 0.2 ML is attributed to a lack of lateral intermolecular interaction, as the nearest intermolecular distance of the second-layer molecules of ~2.68 nm is much larger than the 1.55 nm periodicity of the closely packed F_{16}CuPc stripes.[36] Nevertheless, the DIP:F_{16}CuPc network can serve as an effective molecular nanotemplate to steer the formation of isolated F_{16}CuPc molecular dot arrays.

2. Second-Layer Molecular Chains on a 6P:F_{16}CuPc Binary Network. Similar molecular trapping processes can also be realized on other systems, such as F_{16}CuPc on the 6P:F_{16}CuPc binary molecular network. Figure 3a shows a 30 × 30 nm^2 STM image of a 6P:F_{16}CuPc supramolecular network at a 6P:F_{16}CuPc molecular ratio of 3:1, where all the molecules adopt a flat-lying configuration on the HOPG surface. The unit cell comprising two F_{16}CuPc doublets interconnected by a 6P triplet through intermolecular C−F···H−C hydrogen-bonding is denoted by the rhombus in Figure 3a, with dimensions of c = 2.51 ± 0.02 nm, d = 4.12 ± 0.02 nm, and φ = 90° ± 2°.[26] The rod-like feature represents a single 6P molecule. The proposed molecular packing structure is demonstrated on the left in Figure 3g. It is worth noting that the 6P triplet adopts a face-on configuration here, where the face-on configuration refers to 6P molecules packing with their extending molecular π-planes parallel to the substrate. The intermolecular distance between the neighboring face-on 6P molecules is 0.70 ± 0.02 nm, as shown in Figure 3d. This intermolecular distance is consistent with the previously reported periodicity of 6P monolayers with

dx.doi.org/10.1021/ja106350d |J. Am. Chem. Soc. 2011, 133, 820–825

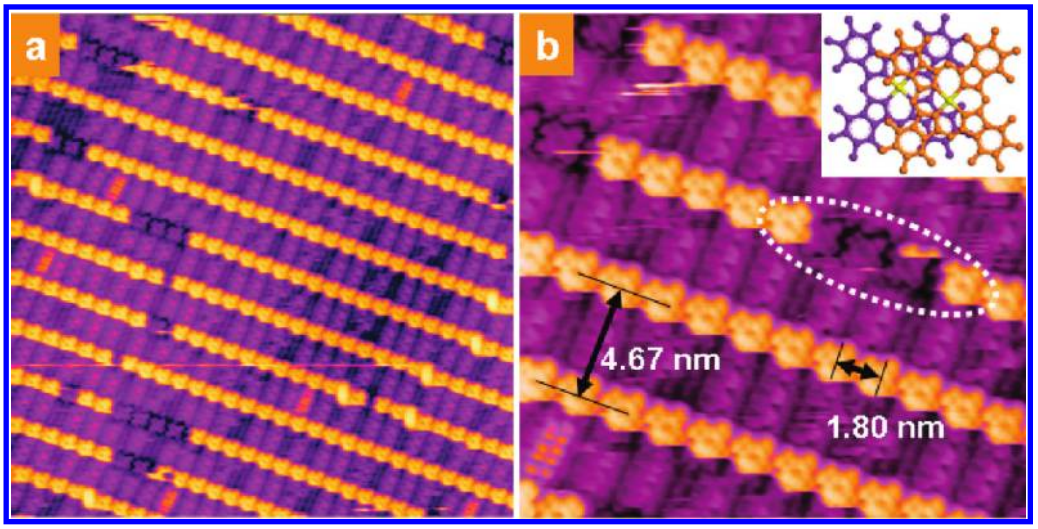

Figure 4. Formation of the second-layer F_{16}CuPc molecular chain arrays: V_{tip} = 2.8 V; (a) 50 × 50 nm^2; (b) 20 × 20 nm^2. The second-layer F_{16}CuPc exclusively adsorbs on top of the underlying F_{16}CuPc molecules, as highlighted by the ellipse in panel b. The top (orange) and the underlying (purple) F_{16}CuPc molecules adopt a slipped geometry, as shown by the schematic drawing in the inset of panel b.

pure face-on configuration on HOPG or other metal substrates.[33,41,42]

It has been demonstrated that the packing structure of a 6P monolayer on graphite is very dynamic.[25,41,42] At high 6P coverage, a more compact 6P monolayer phase could form with periodic insertion of edge-on 6P molecules into the face-on 6P molecular matrix. Here, the edge-on configuration refers to 6P molecules oriented with their phenyl rings perpendicular to the surface and their long molecular axis parallel to the surface. The periodicity of the alternating arrangement of the face-on and edge-on 6P molecules can be adjusted by varying the amount of inserted edge-on 6P molecules.[41] Such control can also be realized in our binary molecular system of F_{16}CuPc with 6P, further increasing the tunability of the binary molecular networks. As shown from Figure 3a to Figure 3b, the random insertion of the edge-on 6P molecules at higher 6P coverage causes the structural rearrangement of the 6P:F_{16}CuPc network. In Figure 3b, the pink rod-like feature represents a single edge-on 6P molecule embedded in the face-on 6P molecules (see details in Supporting Information). The formed F_{16}CuPc linear chain arrays are interconnected, with the single 6P molecular stripes comprising randomly positioned edge-on and face-on 6P molecules via the formation of multiple intermolecular C−F···H−C hydrogen-bonding.

By carefully controlling the 6P coverage, ordered 6P molecular stripes with periodic placement of a face-on 6P dimer and an edge-on 6P monomer can be formed. Such ordered 6P stripes allow the formation of long-range ordered alternating 6P:F_{16}CuPc linear molecular chain arrays, as shown in Figure 3c. Figure 3f displays the line profile taken along the "edge-on + face-on" 6P chain, as marked by the dashed line in Figure 3c, revealing a 1.8 nm periodicity of the 6P molecular chains. The corresponding packing structure is shown in Figure 3e, where two face-on 6P molecules and one edge-on 6P molecule, corresponding to the 1.8 nm periodicity, had also been revealed in our previous report.[31] It is suggested that such periodic arrangements of face-on and edge-on 6P molecules are stabilized by the electrostatic forces between two neighboring types of 6P molecules.[33,41] This is reminiscent of the typical herringbone structure commonly observed in 6P single-crystal solids.[43,44] The F_{16}CuPc chains have the same periodicity of 1.8 nm. The corresponding supramolecular model of the 6P:F_{16}CuPc molecular chain array is shown on the right in Figure 3g, with its unit cell indicated by a dashed rhombus of e = 1.80 ± 0.02 nm, f = 4.67 ± 0.02 nm, and φ = 85° ± 2°. The formation of multiple intermolecular C−F···H−C hydrogen-bonding between neighboring F_{16}CuPc and 6P chains ensures the structural stability of this molecular network.

The rigid 6P:F_{16}CuPc linear chain array can serve as an effective surface nanotemplate to selectively accommodate additional F_{16}CuPc molecules to form second-layer molecular chain arrays, as shown in Figure 4a and its corresponding zoom-in STM image in Figure 4b. The interchain distance of the second-layer F_{16}CuPc chain array is 4.65 ± 0.02 nm, and the intermolecular distance along the F_{16}CuPc chain is 1.80 ± 0.02 nm, exactly mimicking that of the underlying 6P:F_{16}CuPc molecular nanotemplate. The ellipse in Figure 4b highlights an incomplete second-layer F_{16}CuPc chain. This reveals the exclusive adsorption of the second-layer F_{16}CuPc atop the underlying F_{16}CuPc molecules with a small lateral displacement (∼0.50 nm) along the molecular chain direction. The in-plane molecular orientation of the top F_{16}CuPc, i.e., the four-lobe position, is exactly same as that of the underlying one. The inset in Figure 4b displays a proposed molecular packing structure for the F_{16}CuPc bilayer stacking with a slipped geometry. Similar slipped stacking geometry, which maximizes the interlayer $\pi-\pi$ interactions, has been previously observed for closely packed second-layer F_{16}CuPc films on Ag(111)[37] and HOPG,[36] and for the multilayer stacked CoPc thin film on Pb/Si(111).[38] Thus, the exclusive adsorption of the second-layer F_{16}CuPc atop the first-layer ones is also mainly driven by the interlayer F_{16}CuPc−F_{16}CuPc $\pi-\pi$ interactions, and the slipped direction is confined by the underlying molecular chains.

CONCLUSION

Preferential molecular adsorptions on nonporous supramolecular networks have been demonstrated using the model systems of second-layer F_{16}CuPc assembling on DIP:F_{16}CuPc and 6P:F_{16}CuPc supramolecular surface nanotemplates. The arrangement of the second-layer supramolecular nanostructures, individual molecular dots or linear molecular chains, is well controlled by the underlying molecular networks. This suggests a possible

large-scale production method to fabricate organic nanostructure arrays with desired functionality for uses in molecular nanodevices. The interlayer $\pi-\pi$ interactions between the first- and second-layer F_{16}CuPc molecules play important roles in facilitating the preferential adsorptions. Such preferential adsorption on particular molecular sites of a binary molecular template via specific intermolecular interactions could be used as an ideal model system to investigate intermolecular interactions and kinetic growth processes at the atomic scale.

■ ASSOCIATED CONTENT

Supporting Information. Detailed discussion for (1) coaxial alignment of the second-layer F_{16}CuPc molecule with its underlying one on the DIP:F_{16}CuPc template; (2) statistical analysis of the arrangement of the second-layer F_{16}CuPc on the DIP:F_{16}CuPc nanotemplate; (3) lateral profiles of the "edge-on + face-on" 6P molecular stripe. This material is available free of charge via the Internet at http://pubs.acs.org.

■ AUTHOR INFORMATION

Corresponding Author
phycw@nus.edu.sg; phyweets@nus.edu.sg

■ ACKNOWLEDGMENT

The authors acknowledge support from Singapore ARF grants R-143-000-392-133, R-143-000-400-112, and R398-000-056-112 and NUS YIA grant R143-000-452-101. We thank Prof. Jens Pflaum for kindly providing purified DIP molecules and Prof. Chan Yiu Man for helpful discussions on the statistical analysis of the STM images.

■ REFERENCES

(1) Bonifazi, D.; Mohnani, S.; Llanes-Pallas, A. *Chem.—Eur. J.* **2009,** *15,* 7004.
(2) Kudernac, T.; Lei, S.; Elemans, J. A. A. W.; De Feyter, S. *Chem. Soc. Rev.* **2009,** *38,* 402.
(3) Sanchez, L.; Otero, R.; Gallego, J. M.; Miranda, R.; Martin, M. *Chem. Rev.* **2009,** *109,* 2081.
(4) Wan, L. J. *Acc. Chem. Res.* **2006,** *39,* 334.
(5) Mao, J.; Zhang, H.; Jiang, Y. H.; Pan, Y.; Gao, M.; Xiao, W. D.; Gao, H. J. *J. Am. Chem. Soc.* **2009,** *131,* 14136.
(6) Cicoira, F.; Santato, C.; Rosei, F. *Top. Curr. Chem.* **2008,** *285,* 203.
(7) Dil, H.; Lobo-Checa, J.; Laskowski, R.; Blaha, P.; Berner, S.; Osterwalder, J.; Greber, T. *Science* **2008,** *319,* 1824.
(8) Corso, M.; Auwärter, W.; Muntwiler, M.; Tamai, A.; Greber, T.; Osterwalder, J. *Science* **2004,** *303,* 217.
(9) Chen, W.; Wee, A. T. S. *J. Phys. D: Appl. Phys.* **2007,** *40,* 6287.
(10) Stepanow, S; Lingenfelder, M.; Dmitriev, A.; Spillmann, H.; Delvigne, E.; Lin, N.; Deng, X.; Cai, C.; Barth, J. V.; Kern, K. *Nat. Mater.* **2004,** *3,* 229.
(11) Theobald, J. A.; Oxtoby, N. S.; Phillips, M. A.; Champness, N. R.; Beton, P. H. *Nature* **2003,** *424,* 1029.
(12) (a) Staniec, P. A.; Perdigao, L. M. A.; Saywell, A.; Champness, N. R.; Beton, P. H. *ChemPhysChem* **2007,** *8,* 2177. (b) Perdigao, L. M. A.; Saywell, A.; Fontes, G. N.; Staniec, P. A.; Goretzki, G.; Phillips, A. G.; Champness, N. R.; Beton, P. H. *Chem.—Eur. J.* **2008,** *14,* 7600.
(13) Chen, W.; Li, H.; Huang, H.; Fu, Y. X.; Zhang, H. L.; Ma, J.; Wee, A. T. S. *J. Am. Chem. Soc.* **2008,** *130,* 12285.
(14) Madueno, R.; Raisanen, M. T.; Silien, C.; Buck, M. *Nature* **2008,** *454,* 618.
(15) Piot, L.; Silly, F.; Tortech, L.; Nicolas, Y.; Blanchard, P.; Roncali, J.; Fichou, D. *J. Am. Chem. Soc.* **2009,** *131,* 12864.
(16) Zhang, H. L.; Chen, W.; Chen, L.; Huang, H.; Wang, X. S.; Yuhara, J.; Wee, A. T. S. *Small* **2007,** *3,* 2015.
(17) Chen, L.; Chen, W.; Huang, H.; Zhang, H. L.; Yuhara, J.; Wee, A. T. S. *Adv. Mater.* **2008,** *20,* 484.
(18) Bonifazi, D.; Kiebele, A.; Stöhr, M.; Cheng, F.; Jung, T.; Diederich, F.; Spillmann, F. *Adv. Funct. Mater.* **2007,** *17,* 1051.
(19) Lei, S.; Surin, M.; Tahara, K.; Adisoejoso, J.; Lazzaroni, R.; Tobe, Y.; De Feyter, S. *Nano Lett.* **2008,** *8,* 2541.
(20) Calmettes, B.; Nagarajan, S.; Gourdon, A.; Abel, M.; Porte, L.; Coratger, R. *Angew. Chem., Int. Ed.* **2008,** *47,* 6994.
(21) Lu, J.; Lei, S. B.; Zeng, Q. D.; Kang, S. Z.; Wang, C.; Wan, L. J.; Bai, C. L. *J. Phys. Chem. B* **2004,** *108,* 5161.
(22) Kong, X. H.; Deng, K.; Yang, Y. L.; Zeng, Q. D.; Wang, C. *J. Phys. Chem. C* **2007,** *111,* 17382.
(23) Ivasenko, O.; MacLeod, J. M.; Yu. Chernichenko, K.; Balenkova, E. S.; Shpancheko, R. V.; Nenajdenko, V. G.; Rosei, F.; Perepichka, D. F. *Chem. Commun.* **2009,** 1192
(24) Auwärter, W.; Weber-Bargioni, A.; Brink, S.; Riemann, A.; Schiffrin, A.; Ruben, M.; Barth, J. V. *ChemPhysChem* **2007,** *8,* 250.
(25) De Feyter, S.; De Schryver, F. *Chem. Soc. Rev.* **2003,** *32,* 139.
(26) Huang, Y. L.; Chen, W.; Li, H.; Ma, J.; Pflaum, J.; Wee, A. T. S. *Small* **2010,** *6,* 70.
(27) Scudiero, L.; Hipps, K. W.; Barlow, E. *J. Phys. Chem. B* **2003,** *107,* 2903.
(28) Suto, K.; Yoshimoto, S.; Itaya, K. *J. Am. Chem. Soc.* **2003,** *125,* 14976.
(29) De Feyter, S.; Gesquière, A.; Abdel-Mottaleb, M. M.; Grim, P. C. M.; De Schryver, F. C.; Meiners, C.; Sieffert, M.; Valiyaveettil, S.; Müllen, K. *Acc. Chem. Res.* **2000,** *33,* 520.
(30) Lei, S. B.; Yin, S. X.; Wang, C.; Wan, L. J.; Bai, C. L. *Chem. Mater.* **2002,** *14,* 2837.
(31) Hipps, K. W.; Scudiero, L.; Barlow, D. E.; Cooke, M. P. *J. Am. Chem. Soc.* **2002,** *124,* 2126.
(32) Huang, Y. L.; Li, H.; Ma, J.; Huang, H.; Chen, W.; Wee, A. T. S. *Langmuir* **2010,** *26,* 3329.
(33) Chen, W.; Zhang, H. L.; Huang, H.; Chen, L.; Wee, A. T. S. *Appl. Phys. Lett.* **2008,** *92,* 193301.
(34) de Oteyza, D. G.; Krauss, T. N.; Barrena, E.; Sellner, S.; Dosch, H. *Appl. Phys. Lett.* **2007,** *90,* 243104.
(35) Barrena, E.; de Oteyza, D. G.; Dosch, H.; Wakayama, Y. *ChemPhysChem* **2007,** *8,* 1915.
(36) Huang, Y. L.; Chen, W.; Chen, S.; Wee, A. T. S. *Appl. Phys. A: Mater. Sci. Process.* **2009,** *95,* 107.
(37) Huang, H.; Chen, W.; Wee, A. T. S. *J. Phys. Chem. C* **2008,** *112,* 14913.
(38) Chen, X.; Fu, Y. S.; Ji, S. H.; Zhang, T.; Cheng, P.; Ma, X. C.; Zou, X. L.; Duan, W. H.; Jia, J. F.; Xue, Q. K. *Phys. Rev. Lett.* **2008,** *101,* 197208.
(39) (a) Cheng, Z. H.; Gao, L.; Deng, Z. T.; Liu, Q.; Jiang, N.; Lin, X.; He, X. B.; Du, S. X.; Gao, H. J. *J. Phys. Chem. C* **2007,** *111,* 2656. (b) Gao, L.; Deng, Z. T.; Ji, W.; Lin, X.; Cheng, Z. H.; He, X. B.; Shi, D. X.; Gao, H. J. *Phys. Rev. B* **2006,** *73,* 075424. (c) Yim, S.; Jones, T. S *J. Phys.: Condens. Matter* **2003,** *15,* S2631.
(40) Ge, X.; Manzano, C.; Berndt, R.; Anger, L. T.; Kõhler, F.; Herges, R. *J. Am. Chem. Soc.* **2009,** *131,* 6096.
(41) Chen, W.; Huang, H.; Wee, A. T. S. *Chem. Commun.* **2008,** 4276
(42) France, C. B.; Parkinson, B. A. *Appl. Phys. Lett.* **2003,** *82,* 1194.
(43) Koller, G.; Berkebile, S.; Oehzelt, M.; Puschnig, P.; Ambrosch-Draxl, C.; Netzer, F. P.; Ramsey, M. G. *Science* **2007,** *317,* 351.
(44) Baker, K. N.; Fratini, A. V.; Resch, T.; Knachel, H. C.; Adams, W. W.; Socci, E. P.; Farmer, B. L. *Polymer* **1993,** *34,* 1571.